Journal of Alloys and Compounds 480 (2009) 645–649

Contents lists available at ScienceDirect

Journal of Alloys and Compounds

journal homepage: www.elsevier.com/locate/jallcom

Study on morphology and magnetic behavior of $SmCo_5$ and $SmCo_5$/Fe nanoparticles synthesized by surfactant-assisted ball milling

P. Saravanan*, M. Premkumar, A.K. Singh, R. Gopalan[1], V. Chandrasekaran

Defence Metallurgical Research Laboratory, Hyderabad 500058, A.P., India

ARTICLE INFO

Article history:
Received 15 December 2008
Received in revised form 26 January 2009
Accepted 31 January 2009
Available online 10 February 2009

PACS:
75.50.Ww
75.50.Tt

Keywords:
Permanent magnets
Nanostructures
High-energy ball milling
Nanofabrications
Magnetic measurements

ABSTRACT

A surfactant-assisted ball milling was employed for the processing of $SmCo_5$ and $SmCo_5$/Fe nanopowders in presence of oleic acid as surfactant. Two types of samples: one is the sediment powders slightly larger particle size in the range of 0.2–1 μm and other is the suspension in the milling medium with colloidal particles in the range of 4–20 nm were obtained. Structural and magnetic properties of $SmCo_5$ and $SmCo_5$/Fe sediment powders, as well as their constituent colloidal nanoparticles were investigated by a transmission electron microscopy (TEM), small angle X-ray scattering (SAXS) and vibrating sample magnetometer. TEM analysis on the colloidal particles revealed a plate-like faceted morphology with particle diameter in the range of 4–20 nm, while SAXS analysis suggested that the shape of particles are lamellar with average thicknesses in the range of 0.5–1.0 nm. A possible mechanism for the formation of lamellar particles with faceted morphologies due to the milling process is discussed. Magnetic measurements on these nanoparticles showed superparamagnetic nature, with very low coercivity and remanence values.

1. Introduction

Recently, there has been great scientific interest in the preparation and processing of nanocomposite hard magnets [1–3], owing to their capabilities to offer energy-product higher than the traditional, single-phase hard magnets. The basic principle in the nanocomposite hard magnet is to exchange couple a hard magnetic phase having high coercivity with a soft phase of very large magnetization (both the phases must be in nanosize). In this context, the hard magnet research is directed towards development of nanocomposite magnets based on Nd–Fe–B (hard)/Fe (soft), Sm–Co (hard)/Fe (Co) (soft) and FePt (hard)/Fe (soft) phases [4–6], wherein the hard phase provides coercivity and the soft phase offers magnetization. In general, the processing of the nanocomposite magnets are mainly based on mechanical alloying utilizing Fe as the soft phase, as it known to offer very high magnetization. Although, the mixing or alloying of the soft phase, i.e. Fe, with the hard phase such as $SmCo_5$, NdFeB and FePt can be expected with the intensive milling; it should be noted that the mechanical behavior of constituted phases are different—the hard phase being a brittle system, while the soft phase being ductile system. Milling of such dissimilar constituents (brittle–ductile) can greatly affect the size-distribution and hence structural and magnetic properties of the resultant milled nanocomposite powders. Analyzing the structural and magnetic properties of such milled nanocomposite powders can be considered as more of scientific and technological important, in view of improving the performance of nanocomposite magnets. In this context, a systematic investigation on the structural and magnetic properties of $SmCo_5$ (brittle) and $SmCo_5$/Fe (brittle–ductile) magnetic powders has been made utilizing surfactant-assisted milling. The advantages of using surfactant-assisted milling are that one can able to prepare sediment powders, along with very fine colloidal nanoparticles of milling ingredients [7–9].

Generally, irrespective of the synthesis methods, the morphology of nanoparticles is mainly derived with transmission electron microscopy (TEM). Although TEM is a robust instrument in terms of what it can analyze, it does have limitations. One of the largest limitations of TEM is the small sampling volume. When using TEM to analyze the size of a sample, in particular small particles, it is pragmatic to use another technique to corroborate the TEM data. Such techniques would be scattering techniques like small angle X-ray scattering (SAXS) or dynamic light scattering. Scattering techniques sample a larger volume of the specimen and give information about the bulk properties of sample. In the present study, SAXS technique has been applied to study the size, shape and distribution

* Corresponding author. Tel.: +91 40 24586820; fax: +91 40 24340884.
E-mail address: ps@dmrl.drdo.in (P. Saravanan).
[1] Current address: National Institute of Materials Science, 1-2-1 Sengen, Tsukuba, Japan.

0925-8388/$ – see front matter © 2009 Elsevier B.V. All rights reserved.
doi:10.1016/j.jallcom.2009.01.129

of particles from scattering data by means of the well established 'indirect Fourier transformation' technique followed by the numerical deconvolution of the pair distance distribution function (PDDF) [10]. The SAXS results were discussed by comparing with the TEM analysis.

2. Experimental

The precursor $SmCo_5$ alloy was prepared by melting of elemental Sm and Co in high purity argon atmosphere. The alloy ingot was crushed into powder size of ~300 μm, prior to milling. Heptane (99.8% purity) and oleic acid (90%) were used as a solvent and surfactant, respectively during milling. Milling was performed in a planetary ball mill (FRITSCH pulverisette) with the milling vial and balls made of tungsten carbide. A milling duration of 10 h at a constant speed of 200 rpm was used with ball to powder ratio of 10:1. The amounts of surfactant and solvent employed were ~10% and ~55% in weight, respectively of the starting powder. In a similar manner, colloids of $SmCo_5$/Fe nanocomposites were also prepared by mixing 10 wt% of commercially available α-Fe powders (Alfa Aesar; purity: 99.5%) having particle size less than 10 μm.

The use of surfactant during milling resulted in a fine particle suspension (referred as colloid) along with a coarse particles (referred as powder) sedimented at the bottom of the milling vial [8]. Both the colloid and powder were considered for investigation. Microstructure of the colloids was characterized using a TEM equipped with energy dispersive X-ray analysis (EDAX) facility, while for the milled powders a field-emission scanning electron microscopy was utilized. Samples for TEM were prepared by placing a drop of colloid on a Formvar carbon-coated copper TEM grid and subsequently, moving in a dessicator, the so prepared TEM grid in order to dry overnight. The identification of the phases formed in the milled powders was examined by X-ray diffraction (Philips, Cu Kα radiation). Magnetic properties of the powder samples were evaluated using a vibrating sample magnetometer (VSM) (ADE make, model EV9) up to a maximum field of 20 kOe. Small angle X-ray scattering measurements for the $SmCo_5$ and $SmCo_5$/Fe colloidal samples were made with the help of PW3830 X-ray generator (Anton–Paar, Austria) operated at 40 kV and 50 mA with Cu target. The scattering data collected were used to calculate size, shape and distribution of the $SmCo_5$ and $SmCo_5$/Fe colloidal nanoparticles. Data were obtained in the form of scattered X-ray intensity '*I*' as a function of the scattering vector $q = (4\pi/\lambda)\sin\theta$ [1/nm], where θ is the scattering angle and λ is the wavelength of the radiation [11]. The data analysis was performed using GIFT computer program.

3. Results and discussions

By adopting surfactant-assisted milling for the $SmCo_5$ and $SmCo_5$/Fe alloys, both fine powders and their nanoparticle suspension were obtained. The results of structural and magnetic properties of the fine powders, as well as the nanoparticle suspension are discussed below.

3.1. Structural and magnetic properties of $SmCo_5$ and $SmCo_5$/Fe powders

In Fig. 1, we show the SEM morphology of 10 h milled $SmCo_5$ and $SmCo_5$/Fe powders obtained by the surfactant-assisted milling. Though, it can be seen that both the milled powders appear to be large agglomerates with sizes in the range 0.2–1 μm, the presence of plate-like or elongated structures in the case of $SmCo_5$/Fe powders is quite obvious. This is due to the fact that during the milling of brittle ($SmCo_5$)–ductile (Fe) systems, the ductile powders acquire elongated shapes, while the brittle counterparts are simply fractured. The XRD patterns for the $SmCo_5$ and $SmCo_5$/Fe sediment powders obtained surfactant-assisted milling are shown in Fig. 2. The XRD analysis revealed that all the powder samples were mainly comprised of $SmCo_5$ and Fe as the constituent phases, with some traces of impurities such as Sm_2O_3-occurred during the milling process. Using Scherrer's equation, the average grain size of the milled powders was calculated for both $SmCo_5$ and α-Fe phases and is listed in Table 1. In both the milling processes, the calculated grain size values for $SmCo_5$ (1 1 1) peaks were much lower than that of the Fe (1 1 0) peaks. This is due the fact that during milling process, the chances of getting finer grain size for $SmCo_5$ is more prominent, because of its high brittleness, than Fe which is ductile. The magnetic hysteresis curves of the oleic acid coated $SmCo_5$ and $SmCo_5$/Fe

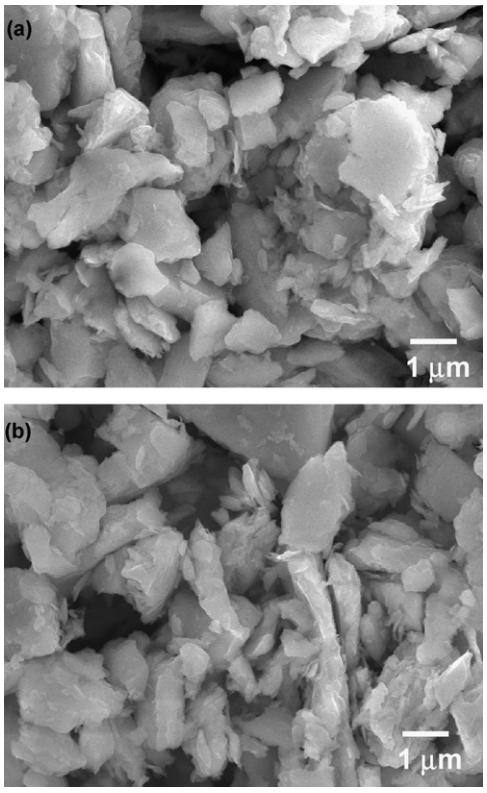

Fig. 1. SEM micrographs of oleic acid coated (a) $SmCo_5$ and (b) $SmCo_5$/Fe nanopowders obtained at 10-h of milling time.

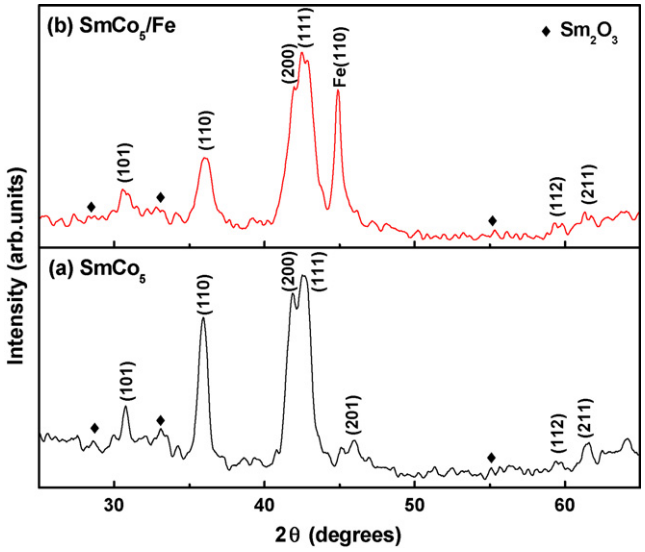

Fig. 2. X-ray diffraction patterns of (a) $SmCo_5$ and (b) $SmCo_5$/Fe nanopowders obtained by surfactant-assisted milling.

Table 1
Properties of 10-h milled $SmCo_5$ and $SmCo_5$/Fe powders obtained by surfactant-assisted milling.

Powders	Grain size (nm)		H_c (kOe)	M_s (emu/g)
	$SmCo_5$ (1 1 1)	Fe (1 1 0)		
$SmCo_5$	19.8	–	5.6	40.9
$SmCo_5$/Fe	21.7	36.8	3.5	54.3

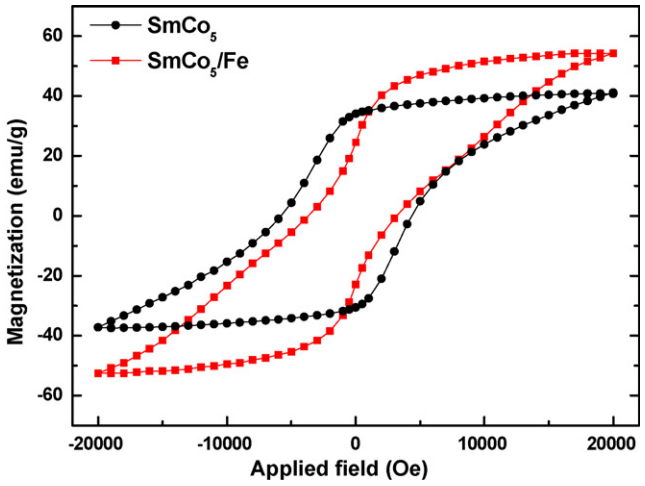

Fig. 3. Magnetic hysteresis loops for the 10-h milled $SmCo_5$ and $SmCo_5$/Fe nanopowders.

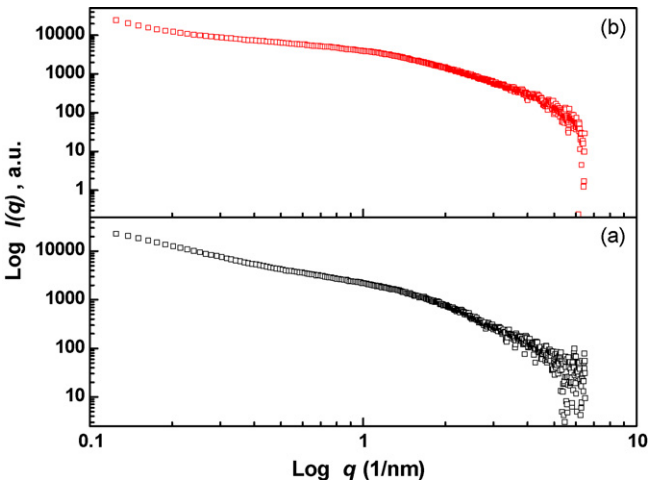

Fig. 5. Plots of the experimental scattering intensity, $\log I(q)$ versus the scattering vector $\log q$: (a) $SmCo_5$ and (b) $SmCo_5$/Fe colloids.

powders are shown in Fig. 3. The measured coercivity (H_c) values of the milled powders were significantly lower than that of their bulk counterparts. This could be due to the particle amorphization occurred in the milled $SmCo_5$ powders [12] and the smaller particles have more amorphous structure, which leads to the reduced coercivity [13]. Further, it is also possible that the oxide impurities (Sm_2O_3) which were formed during milling may contribute to the decrease in coercivity values. The measured H_c values for the $SmCo_5$ powders (5.6 kOe) are relatively higher than that of the $SmCo_5$/Fe powders (3.5 kOe); while, the measured magnetization (M_s) values for the $SmCo_5$/Fe powders (54.3 emu/g) are higher than that of the $SmCo_5$ powders. The above facts are attributed to the addition of soft magnetic phase (Fe) with the $SmCo_5$ phase. A simple calculation of the saturation magnetization value assuming 220 emu/g for Fe and as we know that 10% by weight is iron in the milled powder sample and taking the magnetization of $SmCo_5$ to be 41 emu/g; the obtained magnetization value 54.3 emu/g for the $SmCo_5$/Fe sample confirming that Fe stands alone in the milled sample.

3.2. Structural and magnetic properties of $SmCo_5$ and $SmCo_5$/Fe nanoparticles

With the use of oleic acid together with the heptane during milling, a black coloured magnetic fluid containing nanoparticle suspension was obtained. The surfactant adsorbed by the fresh surface of particles crushed during the ball milling, leading to a surface modification for the ground particles and thereby colloidal nanoparticles were produced. Particle size and morphological studies of oleic acid coated $SmCo_5$ and $SmCo_5$/Fe particles have been studied by TEM and their typical TEM micrographs are shown in Fig. 4. The representative selected area electron diffraction patterns (shown as inset of Fig. 4) indicate the formation of nanocrystallites and can be indexed as $SmCo_5$ and α-Fe phases. The size of the fine particles observed with the TEM was in the range of 4–20 nm. The EDAX analysis also confirms the presence of Sm and Co and Sm, Co and Fe elements in the milled powders of $SmCo_5$ and $SmCo_5$/Fe, respectively. It can be seen that the morphology observed with the TEM is irregular and exhibit plate-like features having one- or two-side faceted morphology.

The experimental scattering function $I(q)$ obtained for the $SmCo_5$ and $SmCo_5$/Fe colloidal samples are shown in Fig. 5, which clearly indicates that the shape of the particles are lamellar, based on the power law [10]. The higher scattering intensity observed in the case of $SmCo_5$/Fe nanoparticles in comparison to that of $SmCo_5$ suggests that the former has larger particle size, which is in accordance with the TEM observations (Fig. 4). The pair distance distribution function, $p(r)$ of the particles was obtained from generalized indirect Fourier transformation of the scattering function:

$$p(r) = \left(\frac{1}{2}\pi^2 A\right) \int q^2\, I(q) \cos(qr)\, \mathrm{d}q$$

where $p(r)$ is the PDDF along a direction perpendicular to the lamellar surface, r is a real space distance (units of nm), q is the scattering

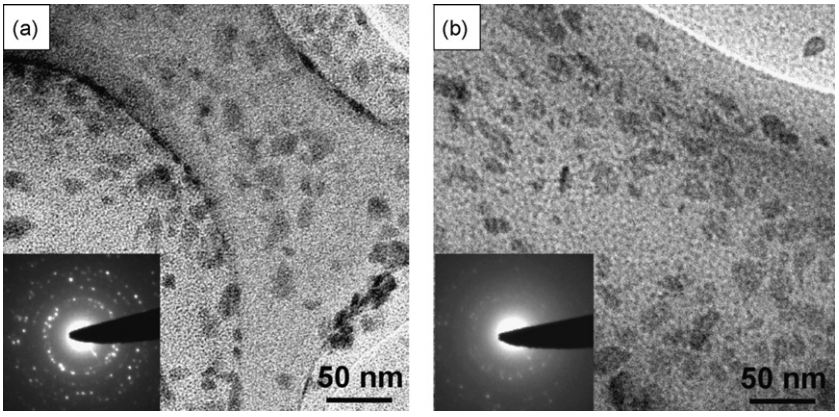

Fig. 4. (a) TEM micrographs of $SmCo_5$ and (b) $SmCo_5$/Fe colloids obtained by surfactant-assisted milling. The insets show the corresponding SAED patterns.

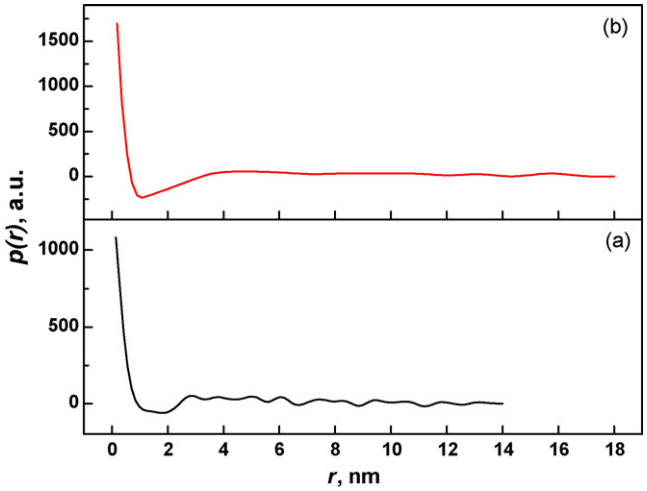

Fig. 6. Plots of the experimental pair distance distribution function $p(r)$ versus radial distance r: (a) $SmCo_5$ and (b) $SmCo_5$/Fe colloids.

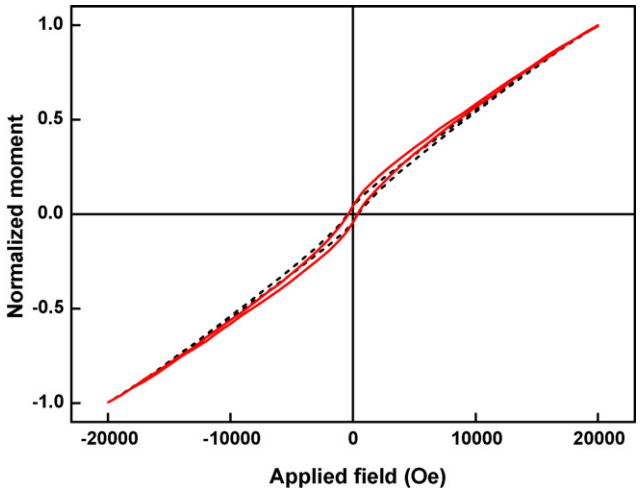

Fig. 8. Room-temperature magnetization loops of surfactant-coated (a) $SmCo_5$ (----) and (b) $SmCo_5$/Fe (—) nanoparticles. Magnetic moment is normalized for maximum saturation value.

vector (0–∞), A is the area of lamella and $I(q)$ is the experimental scattering function.

Fig. 6(a) and (b) shows the $p(r)$ of $SmCo_5$ and $SmCo_5$/Fe colloidal nanoparticles, respectively and it can be seen that the initial slope of both the curves are different; this may be due to different lamellar morphology with different thickness, as well as number of stackings [14]. A thickness of 1 and 14 nm length was observed for the lamellar morphology of $SmCo_5$ nanoparticles; while for the $SmCo_5$/Fe, a thickness of 0.5 nm and length of 18 nm was observed. Since the SAXS results consider a much better statistical average in comparison to that of TEM results, the former exhibit the real size of the particles. Both the samples exhibit the presence of polydispersity, which is also in agreement with the TEM results.

The electron density profiles generated using the program DECON [15], for both the $SmCo_5$ and $SmCo_5$/Fe nanoparticles are shown in Fig. 7. In the case of $SmCo_5$/Fe, the electron density profile shows that the base width values (D) are slightly higher than that of $SmCo_5$ particles. Further, the electron density is not uniform within the nanoparticles and it increases from centre to surface. In general, the electron density will be less at the surface due to the presence of smaller number of atoms [16]. The higher electron density at the surface observed in the present study can be possibly attributed to surfactant coating over the particle surface. The presence of Fe in the $SmCo_5$/Fe sample tends to increase the surface area and reduces the thickness, as can be seen from both the TEM and SAXS results. The increase in surface area can be attributed to the ductile nature of Fe, which is getting more flattened during milling and thereby resulting in a larger surface area for the $SmCo_5$/Fe particles.

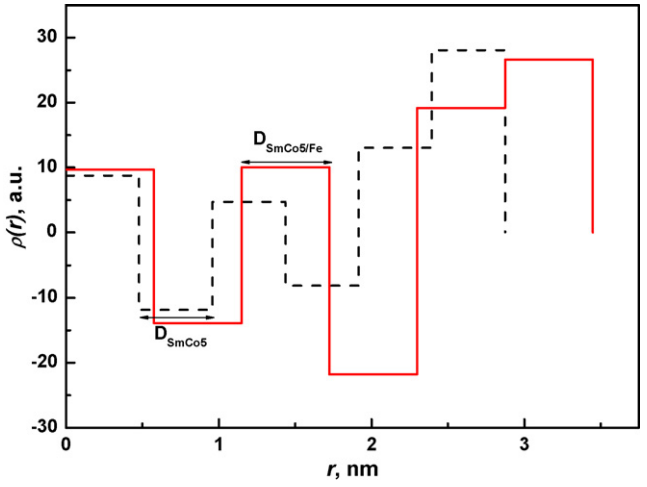

Fig. 7. Plots of electron density distribution $\rho(r)$ versus radial distance r. (a) $SmCo_5$ (----) and (b) $SmCo_5$/Fe (—) colloids.

The lamellar particles with faceted features mentioned above could be possibly produced by fracture of the $SmCo_5$ particles along some preferred crystalline orientation or anisotropic growth of the nanoparticles during the milling. This also indicates the presence of shape-induced anisotropy in the milled powders. The mechanism of ball milling is fairly complex and does not lend itself easily to rigorous theoretical analysis due to its dynamic nature [17]. Low symmetry materials with hexagonal ($SmCo_5$, Sm_2Co_{17} and Co) and tetragonal ($Nd_2Fe_{14}B$) crystal structures have a preferred orientation for fracture due to absence of sufficient number of slip systems [18]. This forms plate-like morphology, which upon further milling would result in the formation of faceted nanoparticles. This may also explain the absence of elongated structures in the $SmCo_5$ samples (as in the case of Fe/FeCo, they have bcc structure).

The magnetic properties of surfactant-coated $SmCo_5$ and $SmCo_5$/Fe nanoparticles using VSM and the results are shown in Fig. 8. Both the hysteresis loops show single-phase-like magnetization behavior—indicating absence of the second phases. It can also be seen from Fig. 8 that these nanoparticles exhibit very low coercivity and remanence values, probably due to the superparamagnetic nature. According to Stoner–Wohlfarth theory [19], in a nanocrystalline hard magnet, wherein the grains are coupled well, the ratio of remanent magnetization M_r to the saturation magnetization M_s (M_r/M_s) will be >0.5. For non-interacting uniaxial single domain particles the remanent magnetic polarization is given by

$$M_r = M_s\langle\cos\theta\rangle$$

where θ is the angle between the saturation direction and the easy axes and $\langle\ \rangle$ denotes an ensemble average. According to the above equation M_r/M_s is 0.5 for an assembly of nanointeracting randomly oriented particles, whereas M_r/M_s is $2/\pi = 0.637$ for microstructures with in-plane random texture. For our oleic acid coated $SmCo_5$ and $SmCo_5$/Fe nanoparticles, the M_r/M_s values are $\ll$0.5; which reveals that these particles are isotropic and non-interacting in nature.

4. Conclusions

Two types of nanostructured materials such as, agglomerates of $SmCo_5$ and $SmCo_5$/Fe powders and their constituent col-

loidal nanoparticles were produced by adopting surfactant-assisted milling. The particle size in the range of 0.2–1 μm was observed for the agglomerates; while for the nanoparticles, it was 5–20 nm. TEM studies revealed a plate-like faceted morphology for the $SmCo_5$ phase; while elongated structures for the Fe phase. The SAXS results obtained in this study are complement with the TEM results, which suggests that the particles are lamellar with average thickness in the range 0.5–1.0 nm. Magnetic measurements on these particles showed superparamagnetic nature with $M_r/M_s \ll 0.5$.

Acknowledgements

The authors thank the Defence Research and Development Organization (DRDO), Government of India for the financial support to carry out this work. The keen interest shown by the Director, DMRL, in this work is also gratefully acknowledged.

References

[1] J. Zhang, S.-Y. Zhang, H.-W. Zhang, B.-G. Shen, J. Appl. Phys. 89 (2001) 5601–5605.
[2] V. Pop, O. Isnard, I. Chicinas, D. Givord, J.M. Le Breton, J. Optoelectron. Adv. Mater. 8 (2006) 494–500.
[3] N.V. Rama Rao, R. Gopalan, M. Manivel Raja, V. Chandrasekaran, D. Chakravarty, R. Sundaresan, R. Ranganathan, K. Hono, J. Magn. Magn. Mater. 312 (2007) 252–257.
[4] G.C. Hadjipanayis, J. Magn. Magn. Mater. 200 (1999) 373–391.
[5] T. Saito, J. Appl. Phys. 99 (2006) 08B522–523.
[6] C.-B. Rong, V. Nandwana, N. Poudyal, J.P. Liu, T. Saito, Y. Wu, M.J. Kramer, J. Appl. Phys. 101 (2007) 09k515–517.
[7] H.G. Cha, Y.H. Kim, C.W. Kim, H.W. Kwon, Y.S. Kang, J. Phys. Chem. C 111 (2007) 1219–1222.
[8] P. Saravanan, R. Gopalan, N.V. Rama Rao, M. Manivel Raja, V. Chandrasekaran, J. Phys. D: Appl. Phys. 40 (2007) 5021–5026.
[9] Y. Wang, Y. Li, C. Rong, J.P. Liu, Nanotechnology 18 (2007) 465701–465704.
[10] O. Glatter, J. Appl. Crystallogr. 10 (1977) 415–421.
[11] O. Glatter, Kratky, Small Angle X-ray Scattering, Academic Press Inc., London, 1982.
[12] C. Suryanarayana, E. Ivanov, V.V. Boldyrev, Mater. Sci. Eng. A 304–306 (2001) 151–158.
[13] R. Gopalan, K. Suresh, D.V. Sridhara Rao, A.K. Singh, N.V. Rama Rao, G. Bhikshamaiah, V. Chandrasekaran, Int. J. Mater. Res. 99 (2008) 773–778.
[14] A. Bellare, H. Schablegger, R.E. Cohen, Macromolecules 28 (1995) 7586–7588.
[15] O. Glatter, B. Hainisch, J. Appl. Crystallogr. 17 (1984) 435–441.
[16] T. Proffen, K.L. Page, R. Seshadri, A. Cheetham, Los Alamos Sci. 30 (2006) 161–163.
[17] C. Suryanarayana, Prog. Mater. Sci. 46 (2001) 1–184.
[18] G.E. Dieter, Mechanical Metallurgy, McGraw-Hill, New York, 1988.
[19] T. Schrefi, J. Fidler, H. Kronmuller, Phys. Rev. B 49 (1994) 6100–6110.